Novel control approach for integrating water electrolyzers to renewable energy sources

Al-sagheer, Yousif; Steinberger-Wilckens, Robert

DOI:
10.1002/fuce.202200066

Received: 26 April 2022 | Revised: 18 July 2022 | Accepted: 22 August 2022

DOI: 10.1002/fuce.202200066

Fuel Cells
From Fundamentals to Systems

RESEARCH ARTICLE

Novel control approach for integrating water electrolyzers to renewable energy sources

Yousif Al-Sagheer PhD | **Robert Steinberger-Wilckens Prof.**

Birmingham Centre for Fuel Cell and Hydrogen Research, University of Birmingham, Birmingham, UK

Correspondence
Y. Al-Sagheer, Birmingham Centre for Fuel Cell and Hydrogen Research, University of Birmingham, Birmingham B15 2TT, UK.
Email: Y.I.W.Al-Sagheer@bham.ac.uk

Abstract

Green hydrogen can be produced by integrating water electrolyzers to renewable energy sources. The integration confronts the problem of renewable power volatility that requires advanced control strategies. There are three main electrolyzer control approaches, which are: battery hysteresis cycle, model-based scheduling, and frequency response. These approaches do not fully solve the problem of electrolyzer operation under power fluctuating conditions. This study introduces a novel integration and control approach for water electrolyzers based on model predictive control algorithm. The algorithm controls electrolyzer load so that steering the system into a breakeven energy balance across the main DC busbar that links generation and demand sides. However, the energy balance is subject to power conditioning losses and capacity constraints of electrolyzer. The novel approach uses simplified prediction models for the generation and demand and introduces a compensator for model uncertainty based on a novel role to the battery as a sensor of energy imbalance. The approach is tested on a 5 kW polymer electrolyte membrane electrolyzer and showed that fully automated energy balancing is achievable for grid connected and stand-alone systems. Also, the electrolyzer can operate at partial capacity with improved efficiency and hydrogen yield, and it is applicable to any mix of renewables.

KEYWORDS

battery as sensor, green hydrogen, model predictive control, model uncertainty compensator, renewable energy fluctuation, water electrolyzer control

1 | INTRODUCTION

Hydrogen production using water electrolyzers is a green source of hydrogen that is anticipated to contribute significantly to decarbonize the transport sector in conjunction with wide adoption of hydrogen-based propulsion systems. The transport sector is considered as one of the major sources of greenhouse gases, for instance, internal combustion engines contribute by around 14% of the greenhouse gases [1, 2]. Fuel cells have promising potentials in electrifying road, maritime, and aviation transport. However, electrification based on fuel cells requires green hydrogen supply in order to be eligible for Renewable Transport Fuel Certificates [3]. Renewable energy industry is a mature technology and the same is true for water electrolysis technology. The integration of these two3 mature

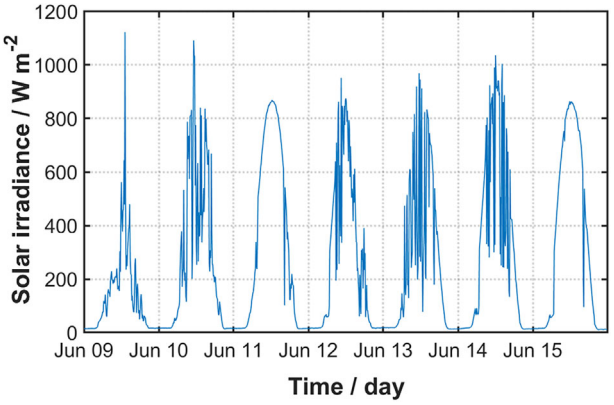

FIGURE 1 Solar irradiance variability.

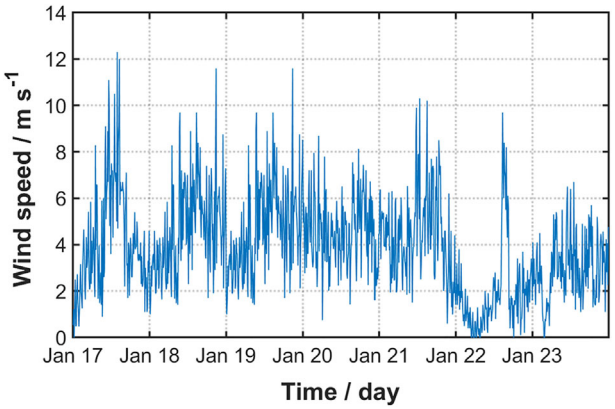

FIGURE 2 Wind speed variability.

technologies, however, is still under research and development. Many pilot projects of hydrogen from renewable energy sources (RES) were installed around the world to investigate the feasibility of the concept and to develop energy management strategies that can handle electrolyzer operation under power volatility of solar and/or wind energy sources [4–12]. The main issue that requires attention is identified as the fluctuated power from RES due to variable wind speed and solar irradiance. The variability can be divided into two components. A deterministic component due to daily profile of solar irradiance or seasonal profile of wind speed, the second is a stochastic component due to different random natural phenomena such as partial shading from clouds [13–15] or sudden changes is the wind speed and its direction or due to any technical fault in the system. The fluctuation rate in the wind speed varies from an order of 0.1 s to minutes [16, 17]. However, power fluctuations of wind turbines are relatively mitigated by the rotor-inertia, but the fluctuation rate would be still of the order of seconds [18, 19]. The fluctuation rate of solar photovoltaic (PV) power could be on the order of seconds to minutes [20]. While the demand side could vary stochastically according to power usage by end users during their daily activities, which can have a predictable profile [21]. Figures 1 and 2 show examples of solar radiation variability and wind speed variability of 7 consecutive days, respectively.

Intensive research has been conducted over the last two decades considering electrolyzer control and integration to RES, mainly focusing on the deterministic component of renewable energy [22–26]. However, the problem of short-term power fluctuations (the stochastic component) has not been fully resolved.

The simplest water electrolyzer integration is the direct coupling to RES. Researchers are considering direct coupling to solar PV only. The concept depends on proper electrolyzer sizing compared to solar PV panel sizing to match electrolyzer voltage–current curve with PV voltage–current curve at maximum point corresponding to different solar irradiance intensities [27, 28]. However, no large-scale demonstration using direct coupling method is reported. On other hand, direct coupling to wind energy is technically infeasible due to alternating power output from wind turbines. Therefore, direct coupling is not considered as a control approach for electrolyzer operation in this study.

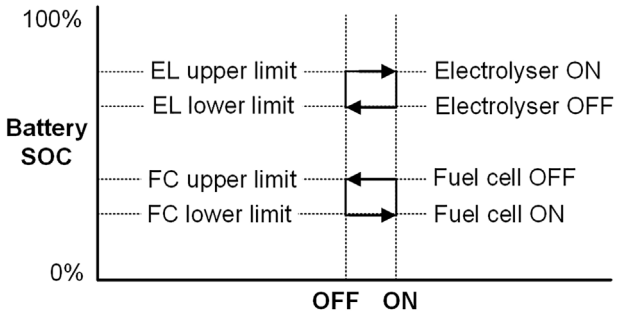

FIGURE 3 Control scheme based on battery hysteresis cycle. EL, electrolyzer; FC, fuel cell; SOC, state of charge.

Three main electrolyzer control approaches can be identified. These are: battery hysteresis cycle, model-based scheduling, and frequency response. In this paper, the three control approaches will be discuss in brief, highlighting the pros and cons of each approach.

1.1 | Battery hysteresis cycle

This method depends on setting upper and lower limits of battery state of charge (SOC). Charging and discharging limits are used for turning ON or OFF the electrolyzer and fuel cell [29], as shown in Figure 3. The SOC can be monitored by measuring the battery voltage and current. The battery is this system reacts as an energy buffer that absorbs power fluctuations and maintains stable powering for the electrolyzer.

The advantage of this approach is the simplicity of the control system. The main disadvantage is that electrolyzer operation is limited to ON/OFF control only. That means operating either at full electrolyzer power with constant efficiency or a complete shutting down. Since the ON/OFF status of the electrolyzer depends on the SOC of the battery, then a large battery size would be required in order to reduce the frequency of swapping between ON and OFF states. If a small battery size is used, then power volatility of RES will result in higher charging and discharging intensity that will hit the limits of SOC more frequently. This will result in more frequent exchange between ON and OFF states of the electrolyzer [30]. Also, the battery will be subject to high number of charging–discharging cycles, and this will reduce the battery life and then higher cost is expected due to the need for battery replacement.

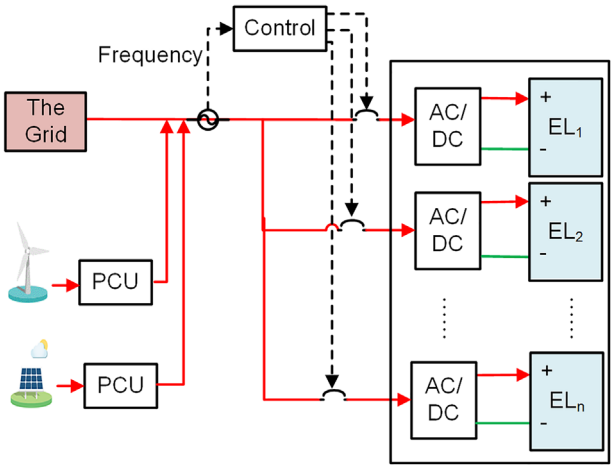

FIGURE 4 Frequency response control scheme. EL, electrolyzer; PCU, power conditioning units.

1.2 | Model-based scheduling

This is an open loop control scheme that depends on the forecast for both renewable power generation and load demand [31–33]. This approach tries to predict the deterministic and the stochastic components of power from RES over a specific future time span, a day ahead, for example. The forecast is based on time intervals of sampling time of 30–60 min, which are relatively long intervals compared to real-time power fluctuation incidents. Therefore, large battery sizes would still be required to absorb and mitigate any power imbalance in the system due to any forecast errors. Another drawback of this approach is operating the system in an off-line mode that could lead to intensive energy drain cycles for the battery, which eventually will reduce the battery life. The forecast is required to be as accurate as possible and therefore complicated prediction methods are used. Some studies estimate the uncertainty as a stochastic model or as a standard deviation of historical data, with adding the uncertainty model to a deterministic model of generation as in Refs. [34–36]. Smoothing out the generation profile is presented in Ref. [37] as a solution to overcome the uncertainty.

1.3 | Frequency response

This approach depends on monitoring the frequency of an AC power source such as the grid. The power is supplied to the electrolyzer from the grid through an AC–DC converter and the energy balance in this case would be implemented on the AC side of the system where electrolyzers can offer grid balancing services [38–40]. Hydrogen gas produced with this approach cannot be considered as fully green fuel because grid energy is a mix of renewable energy and fossil fuel energy from conventional power stations. Therefore, hydrogen produced using this method will have a carbon footprint. For example, the intensity of greenhouse gas emission of electricity generation for European grid is 275 g CO_2 kW h^{-1} in 2019 [41]. Figure 4 shows electrolyzer operation controlled by frequency control scheme. The electrolyzer consists of sub-electrolyzer units, which are turned ON or OFF sequentially while monitoring the frequency (Hertz) of the grid. When the grid is overloaded, the frequency starts to fall, and the electrolyzer is turned OFF. When the grid is underloaded, the electrolyzer receives a signal to turn ON. Therefore, electrolyzer operation is limited to ON/OFF control, and it operates at a constant nominal efficiency. On other hand, power stations on the grid have their own frequency regulators to maintain grid frequency. Furthermore, the challenge with integrating RES to the grid is the lack of inertia, which can lead to rapid frequency variations. Therefore, electrolyzers are required to adapt fast frequency response to support a more secure and resilient grid operation [42, 43]. In addition to ON/OFF control of electrolyzers operation, variable electrolyzer load has been investigated for frequency ancillary services [44, 45].

2 | EXPERIMENTAL APPROACH

The stochastic nature of renewable power generation is a critical problem that needs to be addressed by researchers and engineers. During a given moment of operation, the controller is required to run the fuel cell or the electrolyzer at a specific power load, which is determined by an energy management high-level controller (HLC). In model-based scheduling approach, the HLC relies on a forecast for generation and demand. However, the forecast would always

have a margin of error [46–48]. Furthermore, the forecast is updated at a relatively low sampling rate of 10–30 min compared to actual stochastic variations of order of seconds and sometimes in milliseconds. The mismatch between prediction sampling rate and the actual rate of variation could result in energy imbalance. The control system could adopt a conservative approach [49], where the surplus power is lost or even undetected due to adopting prediction that underestimates the actual generation and hence operates the electrolyzer at load levels much below the actual surplus. On other hand, overestimating the generation could result in operating the electrolyzer at power level more than the actual surplus. Such a situation can lead to fast depletion of the battery or even a system failure. Power intermittency of RES can turn to be a threat to the stability and reliability of power systems as the penetration of renewables increases in the grid. This is because there will be a significant share of fluctuating power sources in the grid [50–52]. Solving these issues requires incorporating a prediction algorithm in the energy balance control and it requires also developing novel methods to deal with the uncertainty of prediction. Also, it requires implementing the energy balance at high sampling rate, so that the system can achieve real-time control. Applying the above two requirements will enable the controller to trace and compensate abrupt and fast stochastic variation in both generation and demand sides. The importance of real-time energy balance has been reported also in many publications [53–56].

2.1 | Novel energy control system

In this work, a novel energy control system is introduced. The novel approach is a control-oriented approach that depends on having an energy storage system as an energy buffer, it is battery in this case. The battery plays a crucial and novel role in the proposed approach. In addition to its fundamental role as an energy buffer, the battery serves as an indicator or a sensor for any power imbalance in the system. The concept relies on that any power contribution from the battery, whether positive or negative, indicates that the system is out of balance in terms of net power incoming and outcoming to and from the DC busbar. In other words, any charging or discharging of the battery indicates that we operate the electrolyzer and the fuel cell at a power level that does not satisfy the energy balance. Also, it indicates that the system is currently deviated from a desired energy balance, which can be defined, for instance, as having a zero-power equilibrium across the DC busbar.

In this study, an energy balance controller is developed. The control system comprises of two levels of control. A low-level controller (LLC) responsible for controlling electrolyzer and fuel cell power to follow a setpoint. The design of LLC of the electrolyzer incorporates compensators for the uncertainty of electrolyzer control model and the uncertainty of control signal law of the DC–DC buck converter, which controls electrolyzer electrical current. Also, electrolyzer electrical current constraints have been considered. The LLCs of the electrolyzer and fuel cell are not addressed in this study as the focus of this study is about the energy balance control. The HLC is responsible for calculating power setpoint for the electrolyzer and fuel cell using prediction models for generation and demand sides [57].

The overall system layout is described in Figure 5. The power balance is implemented on the DC side of the system. Therefore, all the nodes of power sourcing and power sinking connected to the DC busbar will require power conditioning units (PCU), except the battery.

2.2 | Battery role

The control algorithm is based on a novel concept for the battery role in the system. In addition to its role as an energy buffer, the battery is used as a sensor to detect any power imbalance in the system that can result from to any uncertainty in the prediction models. So, the battery contribution will be used for compensating the error in the prediction models. In the system shown in Figure 5, the battery is connected directly to the DC busbar. Such arrangement provides the busbar with energy buffer and will allow the controller to have enough time to respond to power fluctuations. Also, the energy buffer will protect electrical devices connected to the busbar against any abrupt power fluctuations and will maintain the voltage of the busbar at the nominal voltage of the battery. In general, the battery nominal voltage can be chosen to fit a voltage requirement in the system to facilitate interfacing system components. Practically, the busbar voltage needs to be adjusted between the nominal voltage and the charging voltage of the battery in order to ensure high SOC of the battery during system operation. The DC busbar voltage can be regulated by the PCU of generation side. The nominal DC voltage in this study was chosen as 48 V, but the PCU of generation side maintains a voltage of 50 V in order to keep the SOC of the battery around 70% [57, 58].

2.3 | Control algorithm

The controller uses model predictive control (MPC) algorithm to implement the energy balance subject to operational constraints in the system. Developing MPC algo-

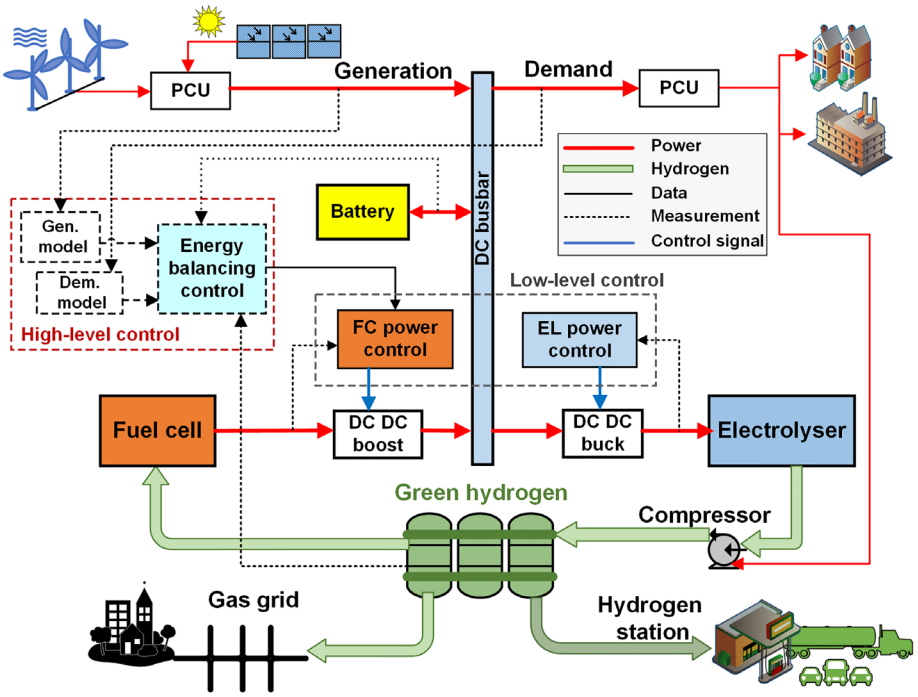

FIGURE 5 Energy control of a hydrogen system integrated to renewable energy sources (RES). EL, electrolyzer; FC, fuel cell; PCU, power conditioning units.

rithm starts with defining the cost function J as in Equation (1) using prediction models for power surplus and power deficit from Equations (2) and (3).

$$\begin{aligned} \min \boldsymbol{J} &= \sum_{i=1}^{N}\left[\left(P_{\mathrm{Sur}*}^{k+i}-\left(\frac{P_{\mathrm{EL,sp}}^{k+i}}{\eta_{c_{\mathrm{EL}}}}\right)\right)^{2}\right. \\ \text{sub.to} & \\ \text{const.} & \\ &\left.+\left(P_{\mathrm{Def}*}^{k+i}-\left(P_{\mathrm{FC,sp}}^{k+i}\times\eta_{c_{\mathrm{FC}}}\right)\right)^{2}\right] \end{aligned} \tag{1}$$

$$P_{\mathrm{Sur}*}^{k+i}=P_{\mathrm{G}*}^{k+i}-P_{\mathrm{D}*}^{k+i}\left(P_{\mathrm{G}*}^{k+i}>P_{\mathrm{D}*}^{k+i}\right) \tag{2}$$

$$P_{\mathrm{Def}*}^{k+i}=P_{\mathrm{D}*}^{k+i}-P_{\mathrm{G}*}^{k+i}\left(P_{\mathrm{G}*}^{k+i}<P_{\mathrm{D}*}^{k+i}\right) \tag{3}$$

This study focuses on controller design, prototyping, and performance testing during power surplus events where only the electrolyzer will be in operation. Therefore, fuel cell operation will be not discussed here and will be not included in the algorithm. The cost function $\boldsymbol{J}$ is then reduced to power surplus term only as in Equation (4) and the introduced term "Comp" represents a compensator for the uncertainty of surplus prediction model.

$$\begin{aligned} \min \boldsymbol{J} &= \sum_{i=1}^{N}\left[\left(P_{\mathrm{Sur}^{*}}^{k+i}-\mathrm{Comp}\right)-\left(\frac{P_{\mathrm{EL,sp}}^{k+i}}{\eta_{c_{\mathrm{EL}}}}\right)\right]^{2} \\ \text{sub.to} & \\ \text{const.} & \end{aligned} \tag{4}$$

where N is the prediction horizon. Since real-time control is targeted in this study, the sampling time is selected to be 50–100 ms. Therefore, the prediction horizon will be in a span of a fraction of a second. During power deficit events, there will be no power surplus and Equation (4) will result in zero electrolyzer power. That means turning OFF the electrolyzer.

The solution of Equation (1) determines power setpoint for operating the electrolyzer. If power surplus prediction is 100% accurate, then electrolyzer power setpoint will match the available surplus; hence, electrolyzer operating power regulated by the LLC will be exactly matching power surplus. However, 100% accurate prediction cannot be guaranteed and there will be always a marginal error in the prediction. Any error in the prediction will results in either operating the electrolyzer at lower or higher power level than the actual surplus. In this case, the battery will be either in charging or discharging state, respectively. That means that the battery can indicate errors of the prediction and not only this, the battery contribution can also be used in quantifying the error (model uncertainty). Equation (4) includes an important term of the compensator that is derived from the battery power. This term compensates for prediction error of the generation and demand models. The novel role of the battery as a compensator in multi-sourcing multi-sinking energy systems was reported in Ref. [59].

Renewable power generation model used here is a very simple model that tries to find the maximum actual power by escalating the prediction by an increment which can be determined and tuned by the controller designer. The escalating model, shown in Equation (5), is based on the latest power measurement on the generation side plus an incremental power increase. While the demand prediction model applies the concept of load following as shown in Equation (6). It is based on the latest power measurement on the demand side. The demand side could include external loads by the end users in addition to internal loads by local system ancillaries such as pumps, control and monitoring system, and the hydrogen compressor.

$$P_{\mathrm{G}*}^{k+i} = P_{G,m}^{k} + \Delta P_{\mathrm{G}}^{+} \tag{5}$$

$$P_{\mathrm{D}*}^{k+i} = P_{D,m}^{k} \tag{6}$$

The escalating model in Equation (5) is based on the concept that any overestimate in predicting the surplus will result in steering the electrolyzer to run at a power level exceeding the actual surplus power. Therefore, the battery will be forced to contribute to balance the system. Since we are considering the battery power as an indication of power imbalance across the DC busbar, then MPC algorithm is designed in this study to consider the battery power as an error/feedback signal to compensate for model uncertainty. The compensator formula is shown in Equation (7)

$$\mathrm{Comp} = G_{\mathrm{p}} P_{\mathrm{B}}^{k} + G_{\mathrm{i}} \int_{0}^{k} P_{\mathrm{B}}^{k} \tag{7}$$

where G_{p} and G_{i} are the proportional gain and integral gain of the error signal (battery power). The overall cost function would be as shown in Equation (8)

$$\begin{aligned} \min \ & \boldsymbol{J} = \sum_{i=1}^{N} \left[\left(P_{\mathrm{Sur}*}^{k+i} - \left[G_{\mathrm{p}} P_{\mathrm{B}}^{k} + G_{\mathrm{i}} \int_{k=0}^{k} P_{\mathrm{B}}^{k} \right] \right) \right. \\ \text{sub.to} \quad & \\ \text{const.} \quad & \\ & \left. - \left(\frac{P_{\mathrm{EL,sp}}^{k+i}}{\eta_{c_{\mathrm{EL}}}} \right) \right]^{2} \end{aligned} \tag{8}$$

Equation (8) can be written also in digitized integrator (summation) form as in Equation (9), which is more compatible to the integrator (accumulator) of a control loop when embedding the algorithm in a controller computer; for example, the control loop in LabVIEW vi driver.

$$\begin{aligned} \min \ & \boldsymbol{J} = \sum_{i=1}^{N} \left[\left(P_{\mathrm{Sur}*}^{k+i} - \left[G_{\mathrm{p}} P_{\mathrm{B}}^{k} + G_{\mathrm{i}} \sum_{k=0}^{k} P_{\mathrm{B}}^{k} \right] \right) \right. \\ \text{sub.to} \quad & \\ \text{const.} \quad & \\ & \left. - \left(\frac{P_{\mathrm{EL,sp}}^{k+i}}{\eta_{c_{\mathrm{EL}}}} \right) \right]^{2} \end{aligned} \tag{9}$$

Equation (9) can be embedded in a controller as it is, and the compensator term will represent the proportional-integral feedback from the battery. From investigating the performance of the controller in the lab, it has been noticed that the summation term can be reduced to include only a short history of battery contribution. Therefore, Equation (9) can be rewritten as Equation (10) or (11), where the span of date history of the battery is determined from the observations of system performance dynamics. This process can also be considered as part of parameters tuning of the controller.

$$\begin{aligned} \min \ & \boldsymbol{J} = \sum_{i=1}^{N} \left[\left(P_{\mathrm{Sur}*}^{k+i} - \left[G_{\mathrm{p}} P_{\mathrm{B}}^{k} + G_{\mathrm{i}} \sum_{k-h}^{k} P_{\mathrm{B}}^{k} \right] \right) \right. \\ \text{sub.to} \quad & \\ \text{const.} \quad & \\ & \left. - \left(\frac{P_{\mathrm{EL,sp}}^{k+i}}{\eta_{c_{\mathrm{EL}}}} \right) \right]^{2} \end{aligned} \tag{10}$$

$$\begin{aligned} \min \ & \boldsymbol{J} = \sum_{i=1}^{N} \left[\left(P_{\mathrm{Sur}*}^{k+i} - \left[G_{\mathrm{p}} P_{\mathrm{B}}^{k} + G_{\mathrm{i}} \left(P_{\mathrm{B}}^{k-h} + \cdots \right. \right. \right. \right. \\ \text{sub.to} \quad & \\ \text{const.} \quad & \\ & \left. \left. \left. \left. + P_{\mathrm{B}}^{k-1} + P_{\mathrm{B}}^{k} \right) \right] \right) - \left(\frac{P_{\mathrm{EL,sp}}^{k+i}}{\eta_{c_{\mathrm{EL}}}} \right) \right]^{2} \end{aligned} \tag{11}$$

The constraints of optimization solver are set to the limits of maximum and minimum operating power of the electrolyzer, as in Equation (12). Also, the rate of change of electrolyzer power can be constrained according to electrolyzer specs of minimum and maximum allowable electrolyzer power change, as shown in Equation (13).

$$P_{\mathrm{EL,min}} \leq P_{\mathrm{EL,sp}} \leq P_{\mathrm{EL,max}} \tag{12}$$

$$\Delta P_{\mathrm{EL,min}} \leq \Delta P_{\mathrm{EL,sp}} \leq \Delta P_{\mathrm{EL,max}} \tag{13}$$

The control algorithm of the entire system is illustrated in Figure 6. The algorithm starts with predicting the power of demand side and the power of generation side from renewables. The prediction is based on the models shown in Equations (5) and (6) and using power transducers installed on the generation and demand sides. The pre-

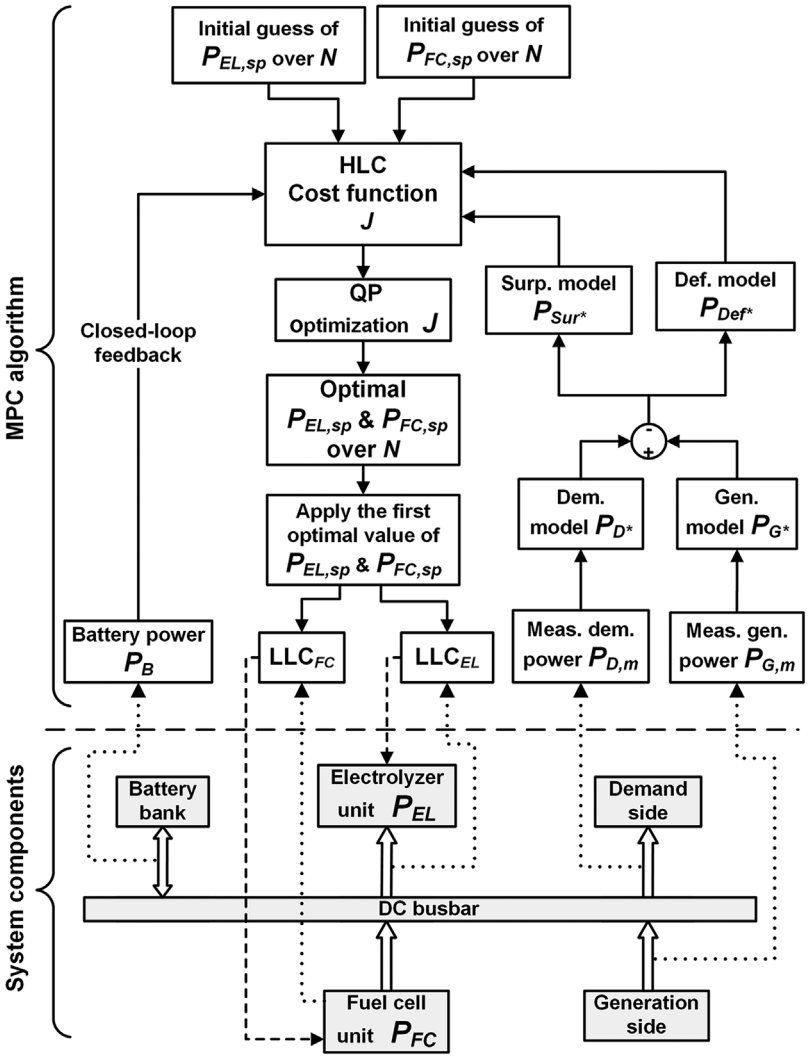

FIGURE 6 Control algorithm using a compensator based on battery power contribution. HLC, high-level controller; LLC, low-level controller; MPC, model predictive control; QP, quadratic programming.

diction models are used to formulate the cost function, which is solved using quadratic programming (QP) solver with initial guess for electrolyzer and fuel cell power. At time zero when the controller starts, the initial guess would be zeros, afterward the guess will be electrolyzer and fuel cell power that is calculated from the previous time step. The QP solver calculates the optimal power level vector for the electrolyzer over the prediction horizon subject to operational constraints of Equations (12) and (13). Only the first value in the vector will be applied to the electrolyzer. If the prediction is very accurate, that is, when the prediction is exactly equal to actual surplus, then the solver calculates electrolyzer power exactly equal to power surplus. Since the algorithm uses escalating model for the prediction then the control loop will reach a point where electrolyzer power exceeds the actual surplus and at this point the battery will contribute to power the electrolyzer. Obviously, this battery contribution is what we need to avoid and to correct by the compensator. That is why the battery contribution is considered here as an error in the energy balance and based on this concept the battery is considered as a sensor for power imbalance in the system.

The compensator formula from Equation (7) will need several sampling times to develop the integral term, which will curtail the overestimated prediction so that the solver calculates electrolyzer power exactly equal to actual surplus despite that the prediction model has already exceeded the surplus. At this point, the escalating process in Equation (5) will stop as a result of the compensation.

3 | RESULTS AND DISCUSSION

The controller performance is tested in the lab using a 5 kW polymer electrolyte membrane water electrolyzer connected to a DC busbar that is interfaced to two randomly emulated profiles for generation and demand sides using a power supply unit and an electron load unit. The generation and demand profiles are shown in Figure 7. As

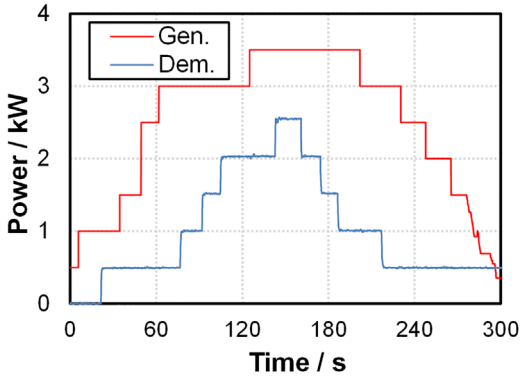

FIGURE 7 Randomly generated profiles for power generation and demand sides.

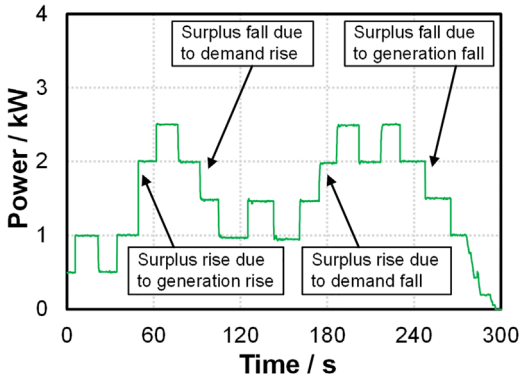

FIGURE 8 Surplus profile with different falling and rising power step changes.

a result of these two profiles, a random surplus profile is created as shown in Figure 8.

The control performance is investigated at different falling and rising power step changes. Four different scenarios are considered, which are:

(i) A surplus rise due to a generation rise
(ii) A surplus fall due to a demand rise
(iii) A surplus rise due to a demand fall
(iv) A surplus fall due to a generation fall

It should be noted that such abrupt changes do not occur commonly in renewable energy systems. However, the controller was tested on extreme power changes in order to prove the concept of the novel control approach of using escalating prediction model as feedforward and the interaction with and the compensator as feedback. On other hand, abrupt changes are expected to occur on the demand side because of any sudden changes in load demand by the end users or because of the hydrogen gas compressor is turned ON.

Figure 9 shows that the controller was able to track power fluctuations in the surplus profile and was able to regulate electrolyzer load accordingly so that the maximum actual surplus energy can be always converted and stored into hydrogen gas. The only disparity between electrolyzer power and the actual surplus power was because of power electronic losses of the DC–DC buck converter which controls electrolyzer load. The converter efficiency was measured to be 94%; therefore, the disparity is around 6%.

TABLE 1 Parameters of model predictive control (MPC) algorithm for high-level control

$\Delta P^{+}_{\text{Gen}}$	100 W (escalating step)
G_{P}	0.2
G_{i}	0.02
$\Delta P_{\text{EL,max}}$	50 W
$\Delta P_{\text{EL,min}}$	−100 W
$P_{\text{EL,max}}$	5000 W
$P_{\text{EL,min}}$	0
$\eta_{c_{\text{EL}}}$	94%
t_{s}	50 ms
N	6

To understand the controller performance, we need to discuss the battery power contribution and the compensator role. Figure 9 shows that the uncertainty of prediction model can be always identified by positive or negative battery power. Whenever the system restores a zero-energy balance and reaches steady state, the compensator is equal to the difference between surplus prediction and the actual surplus, that is the error (uncertainty) of prediction model. This indicates that the compensator can successfully quantify model uncertainty based on battery power contribution.

The controller performance can be tuned using many parameters. Table 1 lists the parameters of MPC algorithm used in the study. Some of these parameters can be used for tuning control performance such as the constraints and the escalation step of the prediction model. Figure 10 shows the electrolyzer response to +500 and −500 W step change to the actual surplus power. Electrolyzer response can be dominated by electrolyzer setpoint calculated from Equation (9), which is constrained by maximum change is electrolyzer setpoint of 50 W per sampling time and a minimum of −100 W per sampling time. Also, the rise time and overshoot can be tunned using the escalating step of prediction model in Equation (5), which was 100 W per sampling time. However, electrolyzer response can also be dominated and tuned by the LLC of the electrolyzer. For example, the rate of change of electrolyzer load can be controlled by setting constraint on the rate of change of electrical current of electrolyzer buck converter. Also, maximum electrolyzer load can be constrained by setting

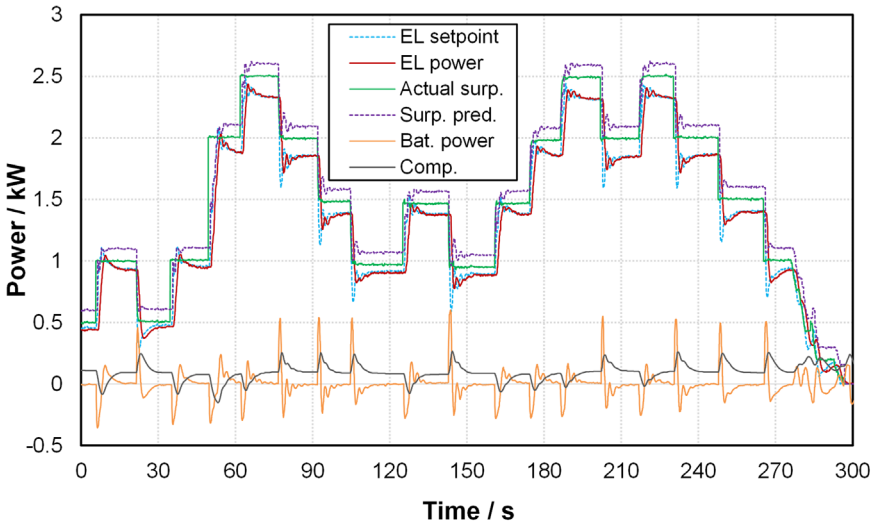

FIGURE 9 Performance of energy system control. EL, electrolyzer.

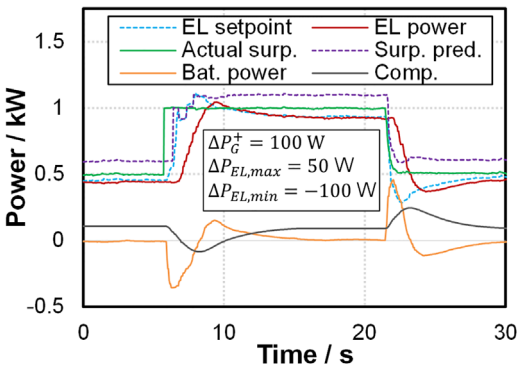

FIGURE 10 Electrolyzer (EL) response to rising and falling surplus power.

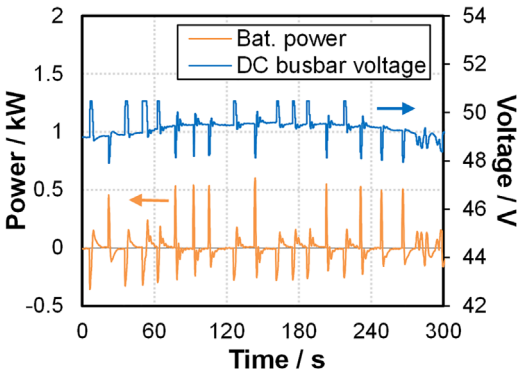

FIGURE 11 DC busbar voltage and battery power contribution.

maximum electrical current that the converter can supply. Detailed interaction between the HLC and the LLC is out of the scope of this paper.

Also, we can see that battery power contributions to the energy balance over the course of system operation were limited to very short intervals only. During these intervals, the feedback of battery power is used for compensating prediction error and as a result restoring zero battery contribution. Hence, the battery plays a role as a sensor to compensate for model uncertainty. Therefore, a small battery size will be required to keep the energy balance and to act as an energy buffer for just a very short time (couples of seconds). The voltage of the DC busbar (which is the same of battery voltage) was maintained within a narrow voltage window, 48–50 V. The slight voltage variations, shown in Figure 11, were because of power imbalance events. A drop in the voltage can be caused by a drop in actual surplus because of either decrease in power generation or increase in load demand. At surplus drop events, the escalated prediction already exceeds the actual surplus; therefore, the compensator will regulate electrolyzer power to match the actual surplus. While a rise in the voltage can be caused by a rise in actual surplus because of either increase in power generation or decrease in load demand. At voltage rise events, the battery is in charging state and the battery power will be negative. In this case and according to Equation (4), the compensator will increase surplus prediction instead of curtailing and at the same time the escalating process can start over again. This will elevate electrolyzer power until an overshoot is detected again by battery contribution (as a discharge now). At this point, the escalating process will be terminated by the compensator and a zero-energy balance will be recovered, therefore.

Figure 12 shows the state of the battery energy during the discharge and charge events. We can see that the battery energy accumulates over the course of the experiment because the busbar voltage was maintained by the PCU of generation side at 50 V, which is higher than the nominal voltage of battery (48 V). With this voltage configuration, the controller will always ensure a high SOC of the battery and the battery energy would be available to act as an energy buffer during any upcoming power transient

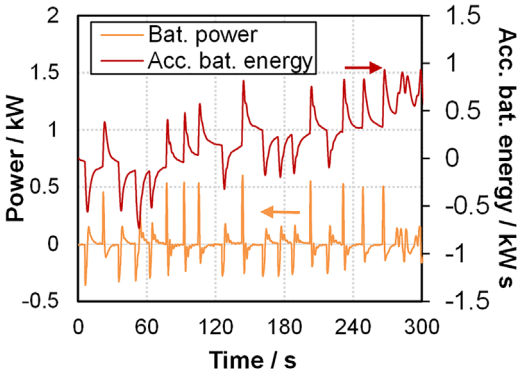

FIGURE 12 Battery power contribution and battery energy accumulation.

event. The energy accumulation will eventually stop when battery voltage reaches 50 V.

4 | CONCLUSIONS

Renewable power variability can be detected and quantified with the novel approach proposed in this study. This will facilitate fully automated electrolyzer operation with applying an energy management including ancillary power needs of the plant. With the novel approach, maximum power availability will be always tracked and converted in the real time into hydrogen. That means that a novel maximum power point tracking (MPPT) algorithm is introduced in this approach, which can be applicable to any mix of RES. As a future work, this requires testing the novel MPPT in the field on a large-scale integration of electrolyzer to a mix of RES, for example, to a solar farm under partial shading and multiple wind turbine machines.

The variable electrolyzer power will result in a higher hydrogen yield due to operating the electrolyzer at higher efficiency region. This will improve overall energy conversion efficiency.

The battery size required in this approach can be very much reduced in comparison to the sizes required in battery hysteresis and model-based scheduling approaches. Therefore, electrolyzer integration at a large scale would be viable and more cost effective (lower capital expenses (CAPEX)). Furthermore, the battery would be no longer subject to high-energy drain cycles as the SOC of the battery can be maintained almost constant. This will prolong the battery lifetime. As a future work also, battery sizing can be well defined by considering the maximum expected change in the load side, which can be equal to hydrogen compressor power. So, the battery nominal power would be equal to the compressor power and the optimal battery size will depend on controller settling time. The settling time in this case will be the time required to restore the energy balance after the compressor load is introduced as a disturbance to the system.

Also, the operating expenses (OPEX) of such systems would be reduced because of applying the energy balance in a fully automated approach. Reduced OPEX will contribute to reducing the cost of hydrogen production. Also, the cost of electricity fed to the electrolyzer is expected to be reduced as the electrolyzer would be located close to RES in a distributed micro-grid system. The cost of electricity transport in the network will be avoided in such distributed integration systems. Therefore, extra reduction in the hydrogen cost can be achieved.

ACKNOWLEDGMENTS

The authors would like to thank the conference committee of European Fuel Cell Forum (EFCF) 2021 for selecting this work to be included in a Special Issue in the Journal "Fuel Cells—From Fundamentals to Systems."

ORCID

Yousif Al-Sagheer PhD https://orcid.org/0000-0002-0429-2456

REFERENCES

1. O. Z. Sharaf, M. F. Orhan, *Renew. Sustain. Energy. Rev.* **2014**, *32*, 810.
2. G. Kalghatgi, *Appl. Energy* **2018**, *225*, 965.
3. Renewable Transport Fuel Obligation, www.gov.uk/guidance/renewable-transport-fuels-obligation **2022**.
4. C. Darras, C. Thibault, M. Muselli, P. Poggi, S. Melscoet, J. C. Hoguet, E. Pinton, F. Gailly, C. Turpin, *Int. J. Hydrogen Energy* **2010**, *35*, 10138.
5. C. Darras, M. Muselli, P. Poggi, C. Voyant, J.-C. Hoguet, F. Montignac, *Int. J. Hydrogen Energy* **2012**, *37*, 14015.
6. O.-S. Parissis, E. Zoulias, E. Stamatakis, K. Sioulas, L. Alves, R. Martins, A. Tsikalakis, N. Hatziargyriou, G. Caralis, A. Zervos, *Int. J. Hydrogen Energy* **2011**, *36*, 8143.
7. T. Nakken, L. R. Strand, E. Frantzen, R. Rohden, P. O. Eide, *Eur. Wind Energy Conf.*, Athens, Greece **2006**, p. 1.
8. T. Schucan, *Final Report of Subtask A : Case Studies of Integrated Hydrogen Energy System* **2000**, p. 1.
9. H. Barthels, *Int. J. Hydrogen Energy* **1998**, *23*, 295.
10. R. Gazey, S. K. Salman, *Proc 41st Int. Univ. Power Eng. Conf.*, Newcastle upon Tyne, United Kingdom **2006**, p. 369.
11. R. Gammon, *Ph.D. Thesis*, Loughborough University (Loughborough, United Kingdom) **2006**.
12. K. Stolzenburg, J. Linnemann, R. Steinberger-Wilckens, *Hydrog. Islands*, Island of Brač, Croatia **2008**.
13. M. Saadsaoud, H. A. Abbassi, S. Kermiche, M. Ouada, *Int. J. Renew. Energy Res.* **2016**, *6*, 413.
14. A. Giyantara, Wisyahyadi, R. B. Rizqullah, Y. T. Kusuma Priyanto, *J. Phys. Conf. Ser.* **2021**, *1726*, 012022.
15. A. Djalab, N. Bessous, M. M. Rezaoui, I. Merzouk, *2018 Int. Conf. Commun. Electr. Eng.*, El Oued, Algeria **2018**, p. 1.
16. J. R. Connell, *Sol. Energy* **1982**, *29*, 363.
17. J. Li, Y. Peng, Q. Yan, *Probabilistic Eng. Mech.* **2013**, *32*, 48.

18. S. G. Varzaneh, G. B. Gharehpetian, M. Abedi, *Electr. Power Syst. Res.* **2014**, *116*, 208.
19. E. Smilden, A. Sørensen, L. Eliassen, *Energy Procedia* **2016**, *94*, 306.
20. M. Eroglu, E. Dursun, S. Sevencan, J. Song, S. Yazici, O. Kilic, *Int. J. Hydrogen Energy* **2011**, *36*, 7985.
21. J.-P. Zimmermann, M. Evans, T. Lineham, J. Griggs, G. Surveys, L. Harding, N. King, P. Roberts, *Household Electricity Survey: A Study of Domestic Electrical Product Usage* **2012**, p. 194.
22. Ø. Ulleberg, T. Nakken, A. Eté, *Int. J. Hydrogen Energy* **2010**, *35*, 1841.
23. J. Bernalagustin, R. Dufolopez, *Int. J. Hydrogen Energy* **2008**, *33*, 6401.
24. E. Dursun, B. Acarkan, O. Kilic, *Int. J. Hydrogen Energy* **2012**, *37*, 3098.
25. C. Azcárate, R. Blanco, F. Mallor, R. Garde, M. Aguado, *Renew. Energy* **2012**, *47*, 103.
26. G. Zhang, X. Wan, *Int. J. Hydrogen Energy* **2014**, *39*, 1243.
27. R. E. E. Clarke, S. Giddey, F. T. T. Ciacchi, S. P. S. P. S. Badwal, B. Paul, J. Andrews, *Int. J. Hydrogen Energy* **2009**, *34*, 2531.
28. L. G. Arriaga, W. Martínez, U. Cano, H. Blud, *Int. J. Hydrogen Energy* **2007**, *32*, 2247.
29. Ø. Ulleberg, *Sol. Energy* **2004**, *76*, 323.
30. O. Ulleberg, *Ph.D. Thesis*, Norwegian University of Science and Technology (Trondheim, Norway) **1998**.
31. F. Garcia-Torres, L. Valverde, C. Bordons, *IEEE Trans. Ind. Electron.* **2016**, *63*, 4919.
32. L. Valverde, C. Bordons, F. Rosa, in *IECON 2012—38th Annu. Conf. IEEE Ind. Electron. Soc.* (Eds: K. Al-Haddad, B.M. Wilamowski), Montréal, Canada **2012**, p. 5669.
33. M. Petrollese, L. Valverde, D. Cocco, G. Cau, J. Guerra, *Appl. Energy* **2016**, *166*, 96.
34. M. Matsubara, G. Fujita, T. Shinji, T. Sekine, A. Akisawa, T. Kashiwagi, R. Yokoyama, in *Proc. 13th Int. Conf. Intell. Syst. Appl. Power Syst. ISAP'05* (Eds: K. Venayagamoorthy, M. Zarghami), Arlington, USA **2005**, p. 67.
35. C.-H. Li, X.-J. Zhu, G.-Y. Cao, S. Sui, M.-R. Hu, *Renew. Energy* **2009**, *34*, 815.
36. G. Giannakoudis, A. I. Papadopoulos, P. Seferlis, S. Voutetakis, *Int. J. Hydrogen Energy* **2010**, *35*, 872.
37. S. G. Tesfahunegn, Ø. Ulleberg, P. J. S. Vie, T. M. Undeland, *Energy Procedia* **2011**, *12*, 1015.
38. J. Eichman, K. Harrison, M. Peters, *Novel Electrolyzer Applications: Providing More Than Just Hydrogen*, Golden, United States **2014**, p. 1.
39. A. Buttler, H. Spliethoff, *Renew. Sustain. Energy Rev.* **2018**, *82*, 2440.
40. X. Li, Y. J. Song, S. Bin Han, *J. Power Sources* **2008**, *180*, 468.
41. Greenhouse Gas Emission Intensity of Electricity Generation, https://www.eea.europa.eu/data-and-maps/daviz/co2-emission-intensity-6#tab-googlechartid_googlechartid_googlechartid_googlechartid_chart_11111 **2021**.
42. M. G. Dozein, A. Jalali, P. Mancarella, *IEEE Trans. Sustain. Energy* **2021**, *12*, 1707.
43. *Fuel Cells Bull.* **2016**, *2016*, 9.
44. F. Alshehri, V. G. Suárez, J. L. Rueda Torres, A. Perilla, M. A. M. M. van der Meijden, *Heliyon* **2019**, *5*, e01396.
45. A. E. Samani, A. D'Amicis, J. D. M. de Kooning, D. Bozalakov, P. Silva, L. Vandevelde, *IET Renew. Power Gener.* **2020**, *14*, 3070
46. S. K. Aggarwal, M. Gupta, *Int. J. Energy Sci.* **2013**, *3*, 1.
47. A. Lahouar, J. Ben Hadj Slama, *2014 5th Int. Renew. Energy Congr*, IEEE, Hammamet, Tunisia **2014**, p. 1.
48. A. Perez-Burgos, R. Roman, J. Bilbao, A. de Miguel, P. Oteiza, *Renew. Energy* **2015**, *77*, 115.
49. L. E. Jones, *Strategies and Decision Support Systems for Integrating Variable Energy Resources in Control Centers for Reliable Grid Operations*, Golden, United States **2012**, p. 1.
50. A. von Meier, *Electric Power Systems: A Conceptual Introduction*, John Wiley & Sons, Inc., New Jersey **2006**, p. 276.
51. W. Kempton, in Renew. Energy Syst. Choice Model 100% Renew. Solut. (Ed: H. Lund), Elsevier Inc., London, United Kingdom **2010**, p. 75.
52. T. D. Tsoutsos, in *Hydrog. Auton. Power Syst.* (Eds: E. Zoulias, N. Lymberopoulos), Springer-Verlag, London, United Kingdom **2008**, pp. 151.
53. A. Basit, A. D. Hansen, P. E. Sørensen, G. Giannopoulos, *J. Mod. Power Syst. Clean Energy* **2017**, *5*, 202.
54. Saving the Planet. Relying on Innovation is Not Enough, https://co2economics.blogspot.co.uk/2016/05/saving-planet-relying-on-innovation-is.html **2016**.
55. S. Sun, M. Dong, B. Liang, *IEEE Trans. Smart Grid* **2016**, *7*, 2337.
56. K. Murphy, S. Schare, in *8th Int. Conf. Energy. Effic. Domest. Appliances Light—EEDAL'15* (Ed: P. Bertoldi), Lucerne, Switzerland **2015**, pp. 1039.
57. Y. Al-Sagheer, *Ph.D. Thesis*, University of Birmingham, Birmingham, United Kingdom **2018**.
58. RS Pro Lead Acid Battery Datasheet 727-0398 (12V100Ah), https://uk.rs-online.com/web/ **2021**.
59. Y. Al-Sagheer, R. Stienberger-Welckins, *GB Patent WO2020188266A1* **2020**.

How to cite this article: Y. Al-Sagheer, R. Steinberger-Wilckens. *Fuel Cells*. **2022**, 1. https://doi.org/10.1002/fuce.202200066